

## The modelling of multi-room air flow and its application to exhaust ventilation analysis

Yuguo Li and Folke Peterson

Dept. of Heating and ventilation  
Royal Institute of Technology  
Stockholm, Sweden.

### Introduction

With the the demand for reducing energy costs and improving air quality in buildings, more attention is being focused on the modelling of infiltration and indoor air flow in multi-room buildings. One characteristic of most existing buildings is that they have floor plans and internal partitioning, which makes the single-cell model redundant. During the last 20 years, several multi-room models have been developed. The Air Infiltration and Ventilation Centre has compared ten mathematical infiltration models and five of them are multi-room models, see Liddament et al (1983). Feustel and Kendon (1985) have also reviewed 15 different multi-room models using a questionnaire. However, these authors have pointed out that most of these programmes are not commonly available to the public, especially the programmes which can be suited to specific needs, such as energy cost analysis and indoor air quality analysis.

The air flow between rooms and between indoor and outdoor is caused by pressure differences, which are affected by wind, thermal buoyancy, the mechanical ventilation system or a combination of these factors. The multi-room building can be considered as a complicated interconnecting system of flow paths. The general method is to present the physical relationship between the pressure difference and the leakage area as the power function. If we assume that there is mass flow balance in every room, we will have a set of nonlinear equations, which can only be solved by iteration. In some programmes for larger openings between rooms, it was not possible to get convergence, see Walton (1982).

The modelling framework described here was carried out to simulate the infiltration, indoor air movement and its interaction with the mechanical ventilation as the first step for studying and indoor air quality. This

paper concentrates on the formulation of the model, algorithms for both indoor pressure distribution and ventilation system analysis, and the question of the influence of infiltration on the exhaust ventilation system in multi-room buildings. The program was named as MIX (multi-room infiltration and exfiltration).

### Multi-room air flow model

The building surfaces and indoor partitions contain openings, either large or small, which permit the air to flow through them whenever there are pressure differences across the opening. The pressure difference may be due to naturally occurring wind, the thermal effects, and the operation of mechanical ventilation.

#### *Wind force and thermal force*

When the path of wind is blocked by buildings, the velocity pressure is converted to static pressure. On the windward side a pressure increase is produced, whereas on the leeward side a pressure drop results. The other side could incur pressure increase or decrease, depending on the wind angle and building shape. This static pressure caused by the wind can be represented by equation (1).

$$\Delta P_w = \frac{1}{2} c_p \rho_o U^2 \quad (1)$$

where

- $\Delta P_w$  = surface pressure due to the wind, Pa
- $c_p$  = wind pressure coefficient
- $U$  = mean wind speed at datum level (building height), m/s
- $\rho_o$  = the density of outside air, kg/m<sup>3</sup>.

Here the pressure produced by the wind is related to the square of the wind velocity. In the present model, the mean wind velocity at building height could be either given or calculated from the meteorological data. If the terrain conditions around the building are known, together with the wind speed at standard conditions, the wind velocity at the building height can be calculated according to the formula

$$U = U_o \cdot \alpha \cdot \left(\frac{H}{H_o}\right)^\gamma \quad (2)$$

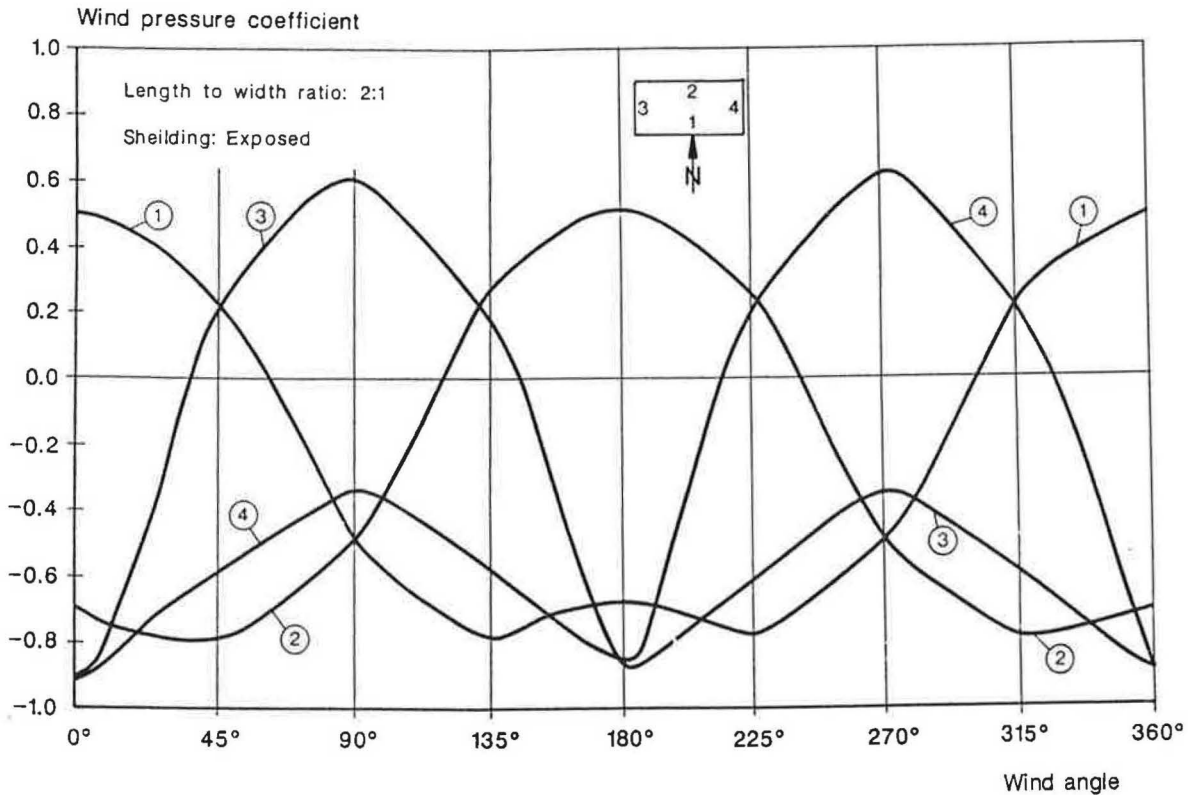


Fig. 1. Wind pressure coefficient data.

where

- $U_0$  = wind velocity at height  $H_0$  in standard conditions, m/s  
 $H$  = building height, m  
 $H_0$  = standard height of wind measurements, 10 m  
 $\alpha, \gamma$  = terrain-dependent coefficient and exponent.

The wind pressure coefficient  $c_p$  is an empirically determined parameter which is assumed to be independent of wind speed but related to the wind direction, the building shape and the shielding conditions. The range of  $c_p$  is between -1.0 and 1.0, where the negative figure expresses the pressure decrease, and the positive figure expresses the pressure increase.

For low building, typically up to 3 stories,  $c_p$  can be considered approximately as an average value for each face of the building for different directions, see Liddament (1986). This is shown in Fig. 1.

Another force causing the pressure difference is the thermal effect. Warm air in a building tends to rise because of its low

density when inside temperature is higher than that outside and vice versa.

The stack pressure, see Fig. 2, can be calculated.

$$p_1 = p_{01} - \rho_1 g h \quad (3.1)$$

$$p_2 = p_{02} - \rho_2 g h \quad (3.2)$$

$$\Delta p = (p_{01} - p_{02}) + (\rho_2 - \rho_1) g h \quad (3.3)$$

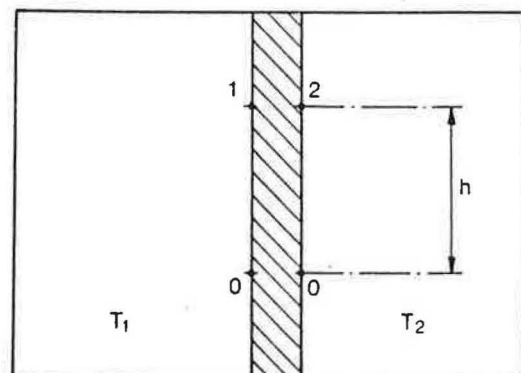


Fig. 2. The stack pressure.

where

- $p_0$  = pressure at datum level  $h^0$ , Pa  
 $g$  = acceleration due to gravity,  $m/s^2$   
 $\Delta p_s = (\rho_2 - \rho_1)gh$  is stack pressure at level  $h$ .

The total pressure difference distribution for envelope surfaces can be obtained from the sum of the wind pressure and stack pressure. The present model adopts the summation formula described by Lillengren (1986), see Fig. 3.

$$\Delta p_{tot}(h) = \left( \frac{1}{2} \cdot c_p \cdot \rho_o \cdot U^2 + \Delta p g \frac{H}{2} - p_i \right) \cdot \left( 1 - \frac{h}{H^*} \right) \quad (4)$$

where

- $\Delta \rho$  = the density difference of the inside and outside air,  $kg/m^3$   
 $H$  = the building height, m  
 $h$  = the height considered, m  
 $H^*$  = neutral level height, m  
 $P_i$  = the internal pressure, Pa.

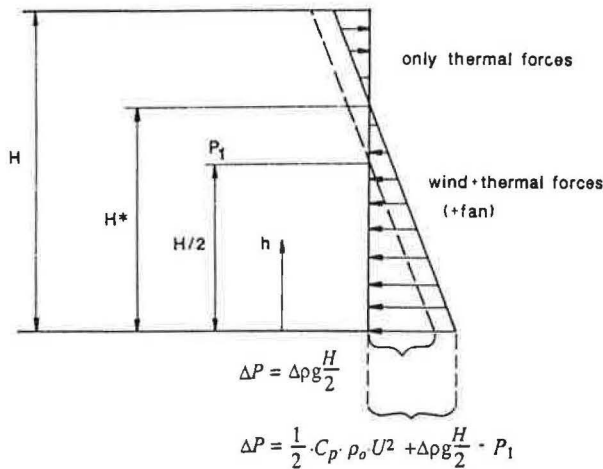


Fig. 3. The pressure across the envelope.

The neutral level height is determined by the following equation,

$$H^* = \left( \frac{1}{2} \cdot c_p \cdot \rho_o \cdot U^2 + \Delta p g \frac{H}{2} - P_i \right) / (\Delta \rho \cdot g) \quad (5)$$

For the building envelope, we should separate the exfiltration and infiltration, which are respectively driven by negative and positive applied pressure difference, depending on the neutral level. In the calculation of the building envelope therefore, three cases were considered,

- o The neutral level is below the floor ( $H^* < 0$ )
- o The neutral level is between the floor and the ceiling ( $0 < H^* < H$ )
- o The neutral level is above the ceiling ( $H^* > H$ )

The pressure difference for internal room surface, for example, room  $i$  and room  $j$ , is

$$\Delta P = P_i - P_j \quad (6)$$

#### Exhaust ventilation system

For the ventilation systems in residential buildings, an exhaust fan is often the most attractive choice because of its low capital and maintenance costs. Traditionally, it is designed with exhaust from bathrooms or kitchens and not from the living rooms or bedrooms. The mechanical exhaust of air pressure will create an internal pressure drop. This additional pressure imbalance could be calculated to treat ventilation as another flow path in which the pressure versus flow rate relationship (the system characteristic) is specified, that is,

$$\Delta p_e = R_e q_e^2 \quad (7)$$

where

- $\Delta p_e$  = pressure loss in the ventilation system, Pa  
 $R_e$  = the resistance of the air way,  $Ns^2/m^8$   
 $q_e$  = volume flow rate,  $m^3/s$ .

The fan characteristic is present by the following equation which gives a good agreement in the normal working mode.

$$p_f = C_1 (1 - C_2 q_f^2) \quad (8)$$

where

- $p_f$  = pressure drop created by fan, Pa  
 $q_f$  = volume flow rate,  $m^3/s$   
 $C_1, C_2$  = fan coefficients.

The intersection of the fan characteristic and the system characteristic will give the point of operation, see Fig. 4. When the internal pressure is changed, the operation point in the exhaust ventilation system will be changed, see Fig. 5.

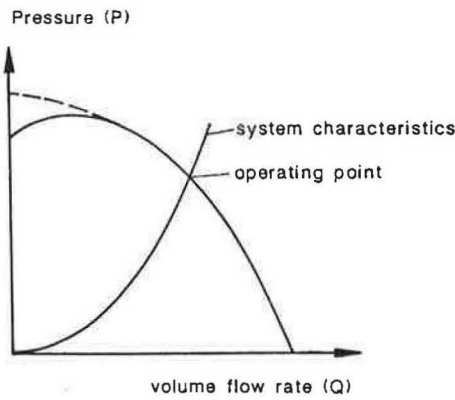
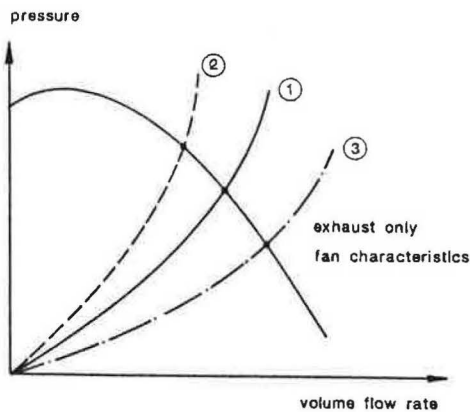


Fig. 4. Fan and system characteristics.



1. Room at atmospheric pressure
2. Room above atmospheric pressure
3. Room below atmospheric pressure

Fig. 5. Room pressure effect on the operating point.

In a ventilation network, the algebraic sum of the pressure drop in any closed mesh should be zero and in any junctions, the mass balance is right. For example, for the exhaust ventilation system illustrated in Fig. 6, the following set of equations can be obtained.

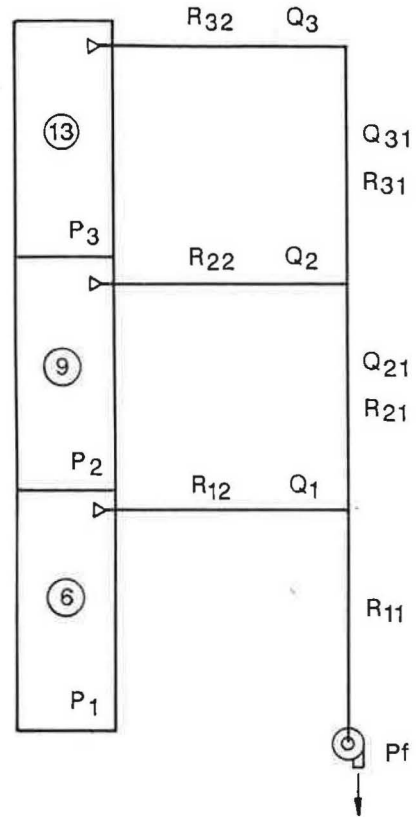


Fig. 6. Exhaust ventilation system.

$$\begin{aligned}
 R_{11}(q_1 + q_2 + q_3) + R_{12}q_1^2 - P_f - P_1 &= 0 \\
 R_{11}(q_1 + q_2 + q_3) + R_{21}(q_2 + q_3)^2 + \\
 R_{22}q_2^2 - P_f - P_2 &= 0 \\
 R_{11}(q_1 + q_2 + q_3) + R_{21}(q_2 + q_3)^2 + (R_{32} \\
 + R_{31})q_3^2 - p_f - p_2 &= 0
 \end{aligned}
 \tag{9}$$

To solve this set of non-linear equations without too many iterations a special method is necessary.

*Flow equations*

For relatively large openings with flow paths, such as the door opening, the following equation based on the orifice turbulent flow is used,

$$q = C_d \cdot A \cdot \sqrt{2\Delta p/\rho}
 \tag{10}$$

where

- $q$  = air flow rate,  $m^3/s$   
 $C_d$  = discharge coefficient  
 $\rho$  = air density,  $kg/m^3$   
 $\Delta p$  = pressure differences across opening, Pa  
 $A$  = area of opening,  $m^2$ .

For a smaller opening, the flow rate,  $q$ , is represent by the power law equation

$$q = k_t (\Delta p)^n \quad (11)$$

where

- $k_t$  = flow coefficient,  $1 m^3/s$  at  $1 Pa$   
 $n$  = flow exponent  
 $\Delta p$  = pressure difference, Pa

The coefficient  $k_t$  is related to the leakage area, and the exponent  $n$  is close to  $2/3$  which agrees with experimental measurements and theretical consideration, see Peterson (1980).

Air flows from high pressure to low pressure. Flow of air into a room (inflow) is defined as positive and flow of air out of a room (outflow) is defined as negative. For each

room, there must be a mass balance.

$$q_e + \sum q_i = 0 \quad (12)$$

where

- $q_e$  = the air flow rate from the ventilation system  
 $q_i$  = the air flow rate across the surface  $i$ .

The balance of the mass flows in all rooms together can be expressed by the following vector equation.

$$f_i(\mathbf{P}) = 0 \quad (i = 1, 2, 3, \dots, N) \quad (13)$$

where

$$\mathbf{P} = (P_1, P_2, P_3, \dots, P_N)$$

$N$  = the number of rooms.

This is a system of non-linear equations, and the number of the equation is equal to the number of the unknown indoor pressure (rooms). This set of non-linear equations can be used to determine room pressure using interation method.

The equations used in MIX are summarised in Table 1.

Table 1. Main equations used in MIX.

Object	Formula
Flow through small openings	$q = k_t (\Delta p)^{2/3}$
Flow through large openings	$q = C_d \cdot A \cdot \sqrt{2\Delta p/\rho}$
Flow through ductwork	$\Delta p_e = R_e q_e^2$
Fan flow characteristics	$p_f = C_1 (1 - C_2 q^2)$
Thermal buoyancy	$\Delta p_s = (\rho_o - \rho_i) g h$
Wind pressure	$\Delta P_w = \frac{1}{2} c_p \rho_o U^2$
Mass balance equations	$q_e + \sum q_i = 0$
Algorithm for nonlinear equations	$P_{new} = P_{old} + \lambda \cdot \delta P$

### Numeric method

This is a description of the numerical method for the ventilation system simulation and the indoor air pressure distribution. These are the two related parts of the procedure for calculating the air flow model.

#### Ventilation system

Initially, considering an airway

$$\Delta P_e = Rq^2 \quad (14)$$

where

$\Delta P_e$  = pressure drop along the air way  
 $R$  = resistance of the airway  
 $q$  = volume flow rate of air.

Thus

$$\frac{d\Delta P_e}{dq} = 2Rq \quad (15)$$

If an initial estimate is made of value the  $q_0$  (it could be obtained from the design data or measuremental data), its error  $\Delta q$  can be determined in the following way.

Approximately, from equation (15)

$$\frac{\Delta(\Delta P_e)}{\Delta q} = 2Rq_0 \quad (16)$$

and it is known from Fig. 7 that

$$\Delta(\Delta P_e) = Rq^2 - Rq_0^2 \quad (17)$$

This means that

$$\Delta q = \frac{Rq^2 - Rq_0^2}{2Rq_0} \quad (18)$$

Now a closed loop  $m$  within a ventilation system network is considered, having  $n$  branches. The above equation could be modified to obtain a correct volume flow rate of air for the mesh considered, which is,

$$\Delta q_m = \frac{\sum_{i=1}^n (R_i q_i^2 - R_i q_{i0}^2)}{\sum_{i=1}^n 2R_i q_{i0}} \quad (19)$$

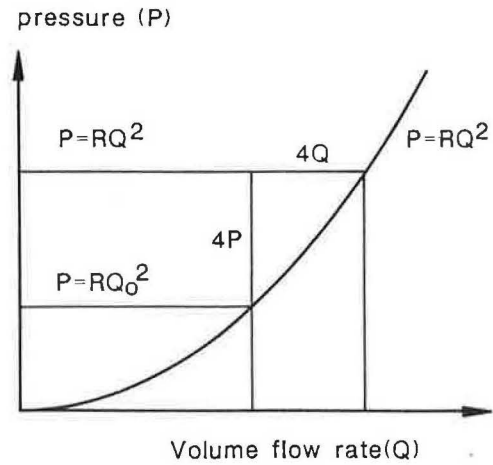


Fig. 7. Numerical analysis of ventilation system.

Since the algebraic sum of the pressure drop in a loop is zero, that is

$$\sum_{i=1}^n R_i q_i^2 = 0 \quad (20)$$

So we can obtain

$$\Delta q_m = \frac{\sum_{i=1}^n (-R_i q_{i0}^2)}{2 \sum_{i=1}^n R_i q_{i0}} \quad (21)$$

If the defined pressure drop is positive in the direction of the flow, then taking into consideration the sign of the pressure drop, the room pressure  $P_m$  and the fan pressure  $P_f$  gives,

$$\Delta q_m = \frac{-\left(\sum_{i=1}^n R_i q_{i0} q_{i0} - P_f - P_m\right)}{\sum_{i=1}^n \left(2R_i q_{i0} - \frac{\delta P_f}{\delta q_f}\right)} \quad (22)$$

where  $P_f$  and  $\frac{\delta P_f}{\delta q_f}$  can be obtained from the characteristic of the fan at the volume flow rate  $q_0$ .

The correct value for the volume flow rate  $q_m$  can be obtained from every room, and it is possible to correct the volume flow rates and repeat the above procedure until all the values of  $q_m$  are below a prescribed level, for example,  $1 \cdot 10^{-4} \text{ m}^3/\text{s}$ .

Therefore, once the internal air pressure distribution is known, the air flow rate from the ventilation system can be calculated.

#### Internal pressure distribution

When it is decided to use one interactive method, two factors should be considered. One is the convergence; the other is the length of calculation times. To prevent long calculation times, it is necessary to develop fast algorithms and estimate the initial values as near to real values as possible. This depends on analysis rather than numerics.

The present calculation adopted different ways to estimate initial values in different calculation conditions.

- o If all the flow exponents are replaced with 1, then a linear equation can be obtained. The solution of the linear equation set is the first set of estimated values.
- o If the inter-room openings are larger than the envelope openings, then the internal air being uniform. In these circumstances the result of a single-cell model calculation are used as the initial value of the multi-room model. The more rooms there are, the more efficient the method.
- o If the air flow for different outside air temperature is calculated at the same wind speed and direction with the same shielding and terrain conditions, the result of the temperature  $\theta_1$  can be used as the initial value of temperature  $\theta_2$ . This is providing that about  $\theta_1 - \theta_2 < 10^\circ\text{C}$

Around the neighbourhood of initial values  $P$ , each of the function  $f_i$  in equation (13) can be expanded by the Taylor series.

$$f_i(P + \delta P) = f_i(P) + \sum_{j=0}^N \frac{\delta f_i}{\delta P_j} \delta P_j + O(\delta P^2) + \dots \quad (23)$$

By neglecting terms of order  $\delta P^2$  and higher, a set of linear equations for correction  $\delta P$  is obtained. This makes each function  $f_i$  closer to zero simultaneously. That is

$$\sum_{j=0}^N \frac{\delta f_i}{\delta P_j} \delta P_j = -f_i(P) \quad (i = 1, 2, \dots, N) \quad (24)$$

We can solve this using the Gauss-Jordan method.

Then

$$P_{new} = P_{old} + \lambda \cdot \delta P \quad (25)$$

where

$$\lambda = \text{relaxing factor } (0 < \lambda < 1)$$

The air volume flow rate from the ventilation system needed in equation (13) is calculated using the method described in the previous section.

The process is iterated to convergence which means that both functions  $f_i$  and variables  $P_i$  have converged.

$$f_i(P_{new}) < \varepsilon$$

$$\frac{P_{new} - P_{old}}{P_{new}} < \varepsilon$$

For a large opening between rooms (for example, when a door is open), the pressure difference is small. This is a potential source of trouble in solving the above linear equation sets using the Newton-Rapson method or its revisions, as described above,

where the derivatives  $\frac{\delta f_i}{\delta P_j} \cdot \Delta P_{n-1}$  must be calculated. Calculations show that the flows corresponding to small pressure differences can not be casually neglected to avoid division by zero. This is because the flows could be large due to a large leakage area, although the pressure difference is very small. Thus it seems that the lower the pressure difference limit to be neglected, the better. The present calculations chose

$$\Delta P_{limit} = 1 \cdot 10^{-10} \text{ Pa}$$

This is a reasonable value, even for a large opening like an open door ( $2 \text{ m}^2$ ). The air flow rate will be less than  $1 \cdot 10^{-6} \text{ m}^3/\text{s}$ , which is small enough to be neglected. In such a case, less than 10 interactions are required ( $\lambda=0.5$ ) for a 13 rooms model calculation. The above discussion could be a solution to the problem proposed by Walton (1982), where even a case with  $0.186 \text{ m}^2$  opening between rooms proved impossible to simulate.

### An example house

A study of the air flow simulation and especially the influence of infiltration on the exhaust ventilation system was done using an example house. The floor plans are shown in Figs 8, 9 and 10. Fig. 11 is a section of the building. There is a total area of  $450 \text{ m}^2$  on all three floors, and a volume of  $1125 \text{ m}^3$ .

An example exhaust ventilation system was designed from rooms 6, 9, 13, which were considered as kitchens or bathrooms, whereas the others were considered as living rooms or bedrooms, see Fig. 6.

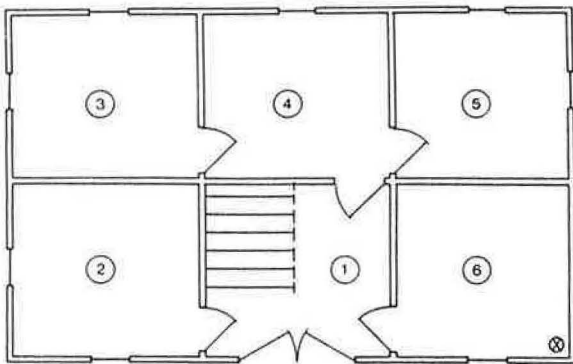


Fig. 8. First floor plan.

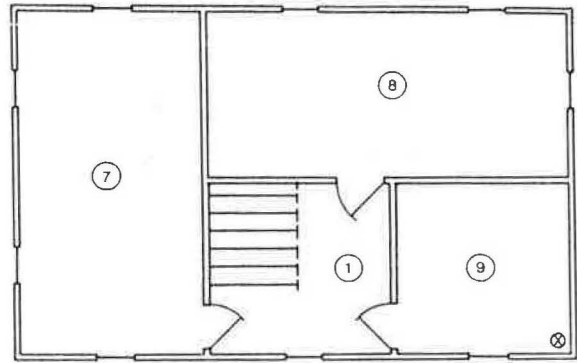


Fig. 9. Second floor plan.

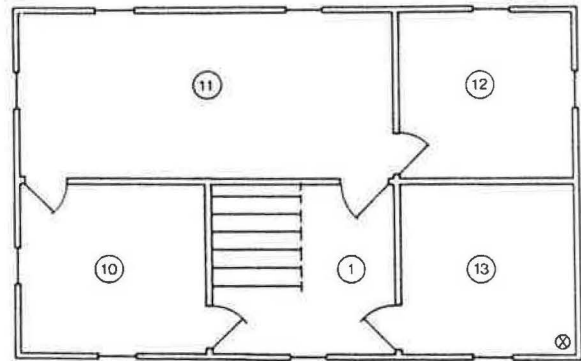


Fig. 10. Third floor plan.

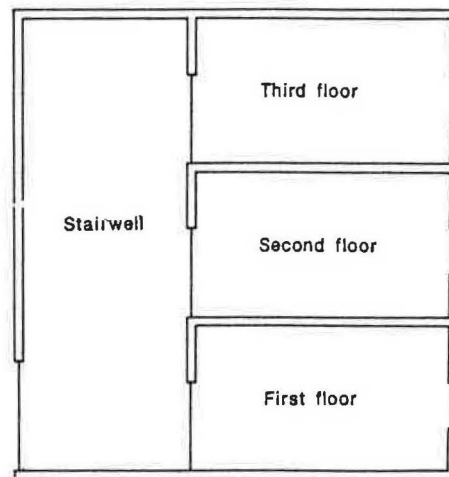


Fig. 11. Section of the example building.



## Result and discussions

### *Underpressure created by the exhaust system*

Operation of the mechanical exhaust ventilation system results in the reduction of an internal pressure or underpressure. When all the inter-room doors are open, there is a uniform internal underpressure, see Fig. 12. In this case, the single-cell model can be used to calculate the air change rate accurately and quickly. When the inter-room openings are smaller, the internal pressure distribution will not be completely uniform. Fig. 13 shows the calculated result when the interroom doors are almost closed. Fig. 15 shows the result when the doors are closed completely,  $k_t$  as 0.0002 as others. The largest indoor pressure difference between two neighbouring rooms can be as high as 10

$P_a$  in the example house. This non-uniform pressure distribution will obviously affect the infiltration, indoor air movement.

The calculation of a single-cell model showed that when all the doors are open and assuming that every face of the building is exposed to the same degree of local shielding and symmetrical leakage conditions, the influence of the symmetrical wind direction on the indoor air pressure and infiltration is small, see Danielson et al (1987). For the multi-room model, however, the result is different. The present calculation shows that if the inter-room flow resistance distribution is unsymmetrical due to the different room sizes, location of doors, and inlet of the mechanical ventilation system, the symmetrical wind direction ( $\theta = 0^\circ$  and  $\theta = 180^\circ$ ) are two examples illustrated in Figs. 13 and 14), also causes different indoor pressure distributions and infiltration.

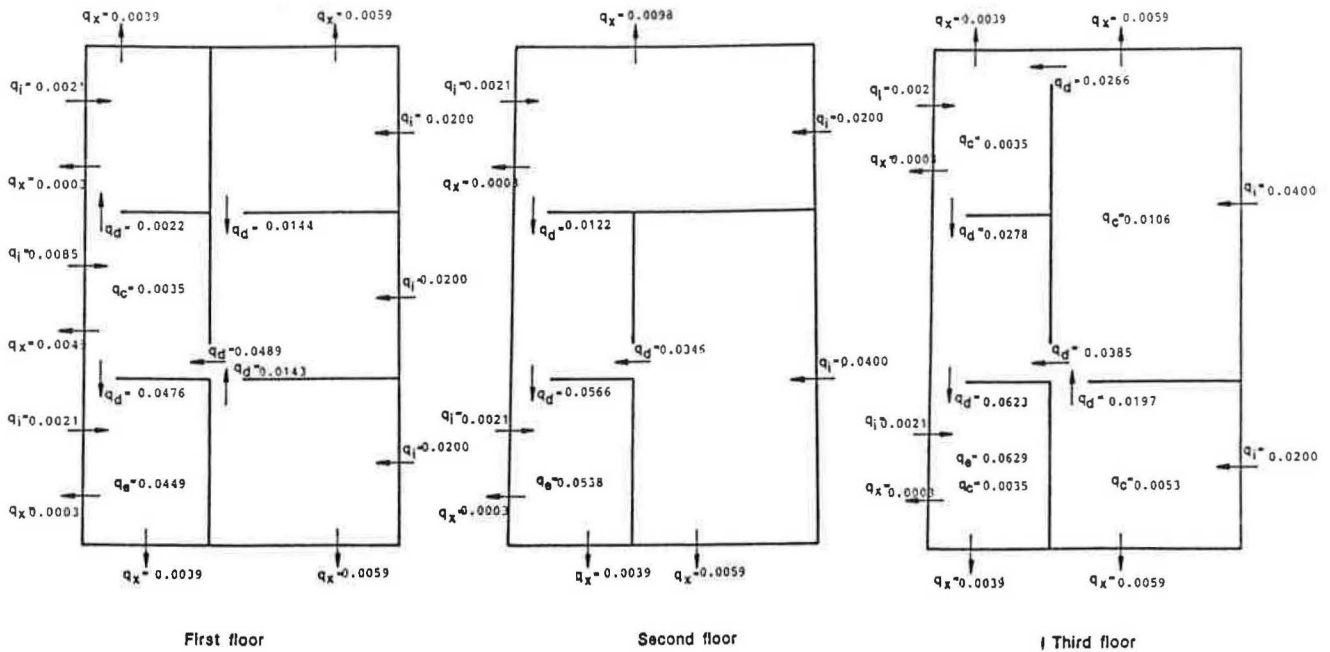


Fig. 12. Infiltration rates, exfiltration rates, ventilation flow rates, and indoor air flow rates,  $\theta_{in} = 20^\circ\text{C}$ ,  $\theta = 0^\circ$ ,  $U = 4 \text{ m/s}$ ,  $\theta_{out} = -10^\circ\text{C}$ ,  $k_t = 0.0002$ , all doors are open.

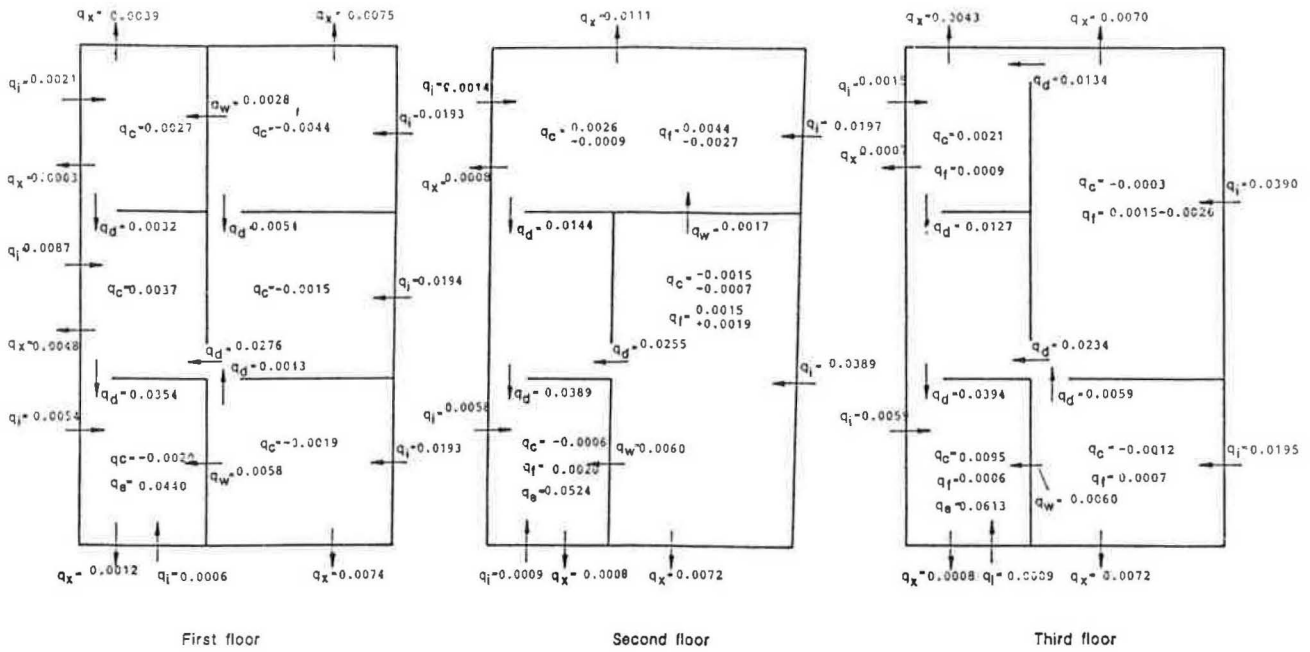


Fig. 13. Infiltration rates, exfiltration rates, ventilation flow rates, and indoor air flow rates,  $\theta_{in} = 20^\circ\text{C}$ ,  $\theta = 0^\circ$ ,  $U = 4 \text{ m/s}$ ,  $\theta_{out} = -10^\circ\text{C}$ ,  $k_t = 0.0002$ , all doors are almost closed.

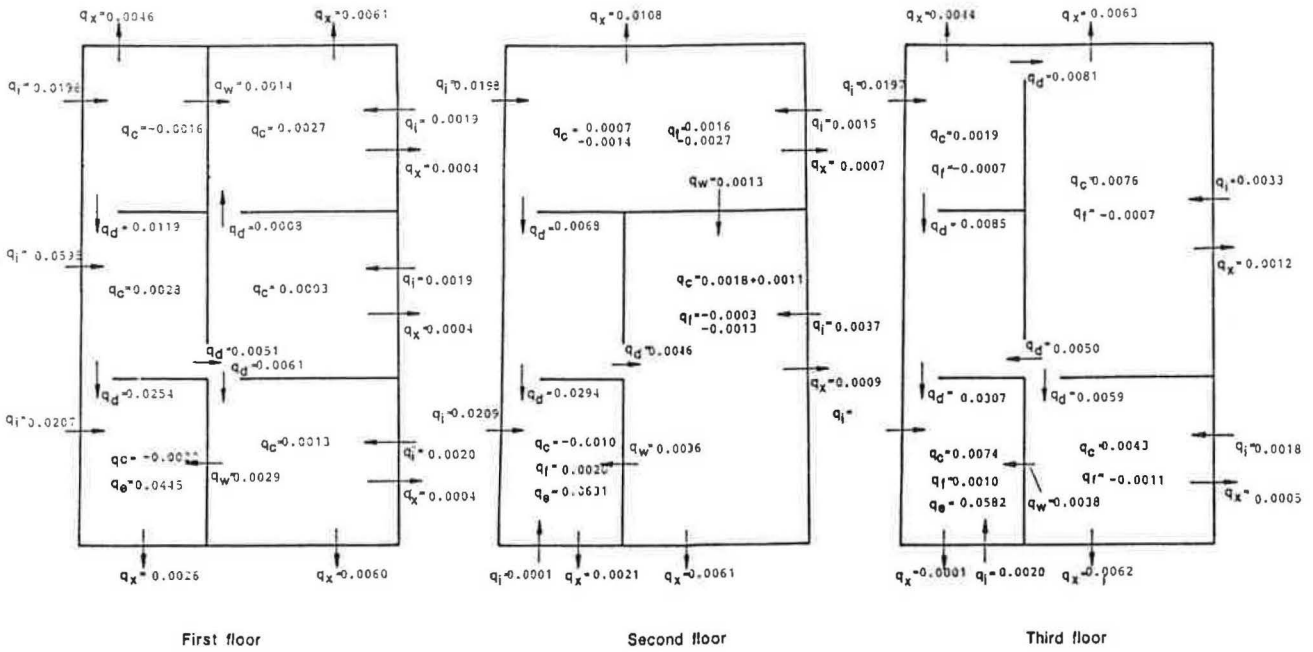


Fig. 14. Infiltration rates, exfiltration rates, ventilation flow rates, and indoor air flow rates,  $\theta_{in} = 20^\circ\text{C}$ ,  $\theta = 180^\circ$ ,  $U = 4 \text{ m/s}$ ,  $\theta_{out} = -10^\circ\text{C}$ ,  $k_t = 0.0002$ , all doors are almost closed.

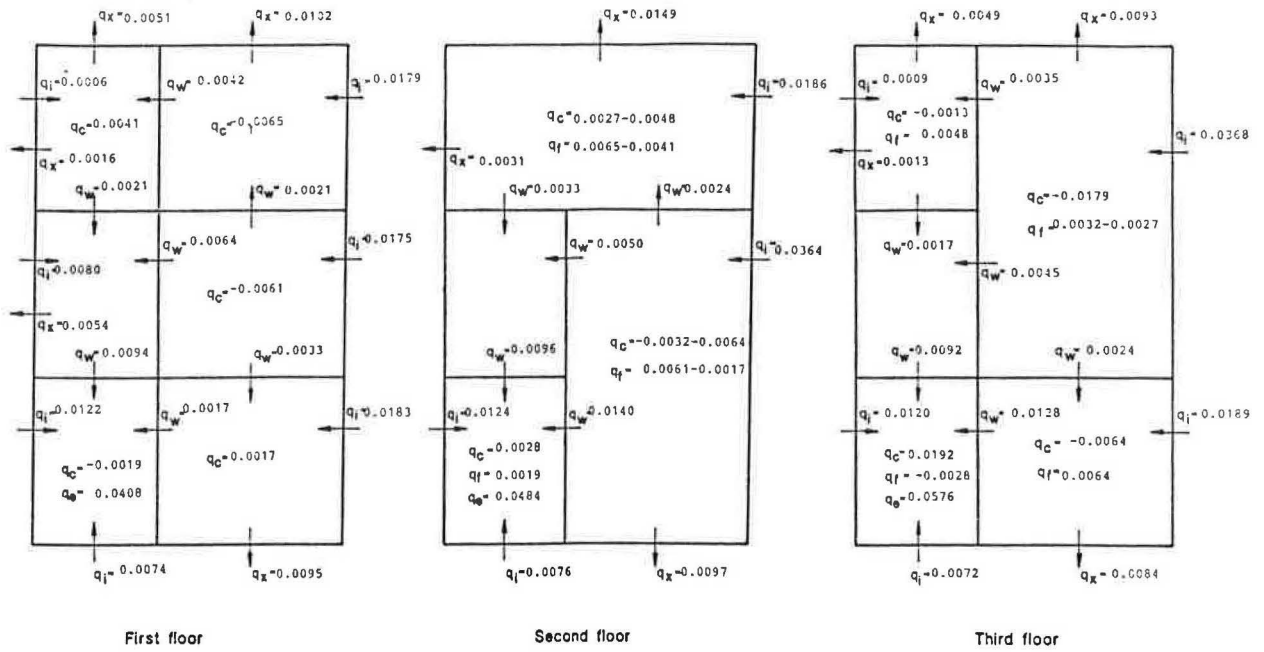


Fig. 15. Infiltration rates, exfiltration rates, ventilation flow rates, and indoor air flow rates,  $\theta_{in} = 20^{\circ}\text{C}$ ,  $\theta = 0^{\circ}$ ,  $U = 4 \text{ m/s}$ ,  $\theta_{out} = -10^{\circ}\text{C}$ ,  $k_t = 0.0002$ , all doors are closed.

*Exhaust ventilation rate*

In different conditions, the exhaust ventilation rate will change from the design data due to the changing of the indoor air pressure. Fig. 16 gives the effect of room pressure on the exhaust fan total pressure. If room pressure is above atmospheric pressure then the exhaust total pressure will decrease, and the exhaust ventilation will increase, see Fig. 5. Conversely, if the room pressure is below atmospheric pressure, an increase in exhaust fan total pressure will result, and the exhaust ventilation rate will decrease, see Fig. 5, again. Figs. 17, 18, and 19 show the influence of  $k_t$ , status of the internal doors and outside temperature on the changing of the exhaust ventilation rate. The common point was that the exhaust ventilation rate decreased when the wind speed increased because the indoor pressure decreased. Closing an internal door, related to the ventilated room, tightening the envelope, or a reduction in the outside temperature will cause the exhaust ventilation rate to decrease.

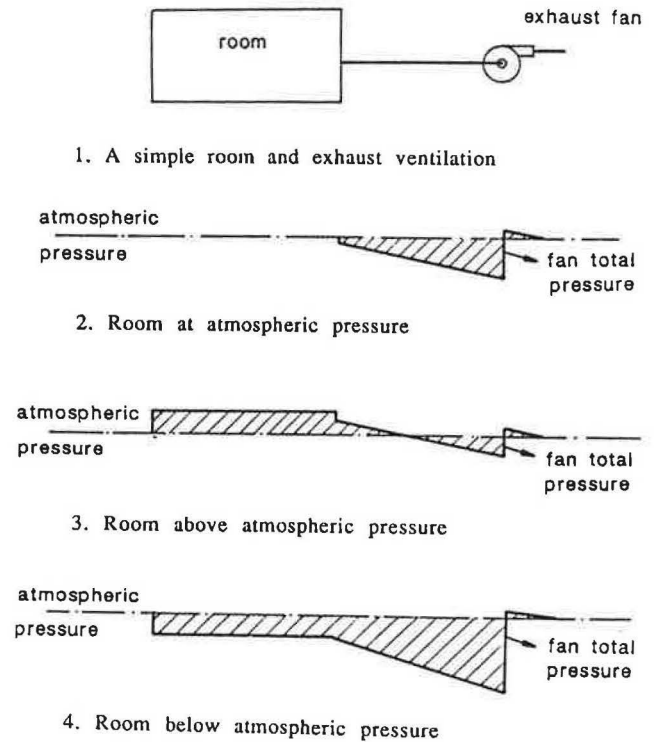


Fig. 16. Effect of room pressure on exhaust ventilation.

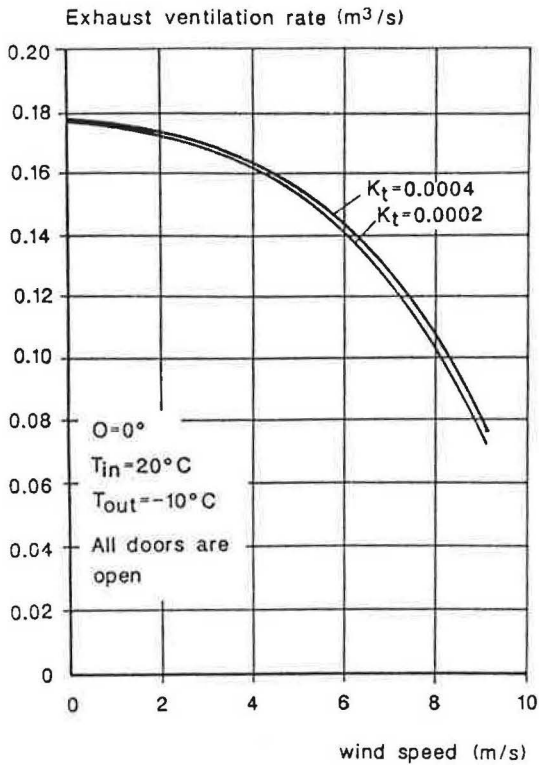


Fig. 17. The changing of the exhaust ventilation flow rates for different  $k_t$ -values.

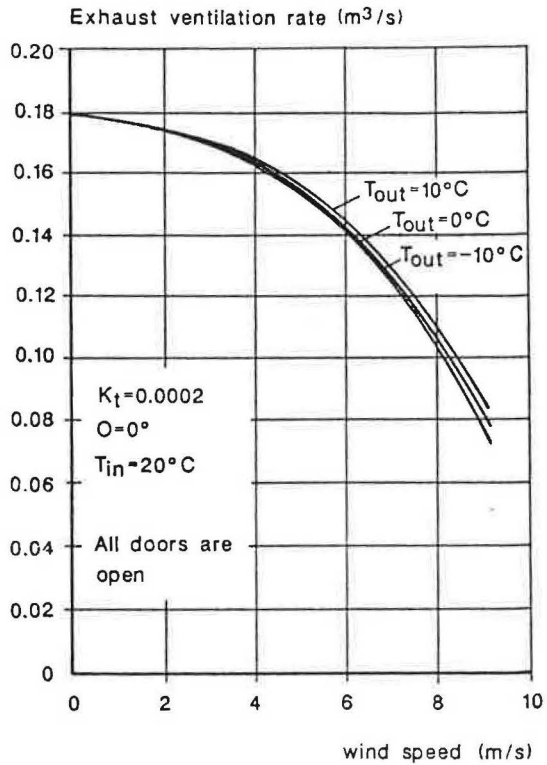


Fig. 19. The changing of exhaust ventilation flow rates for different outdoor temperature.

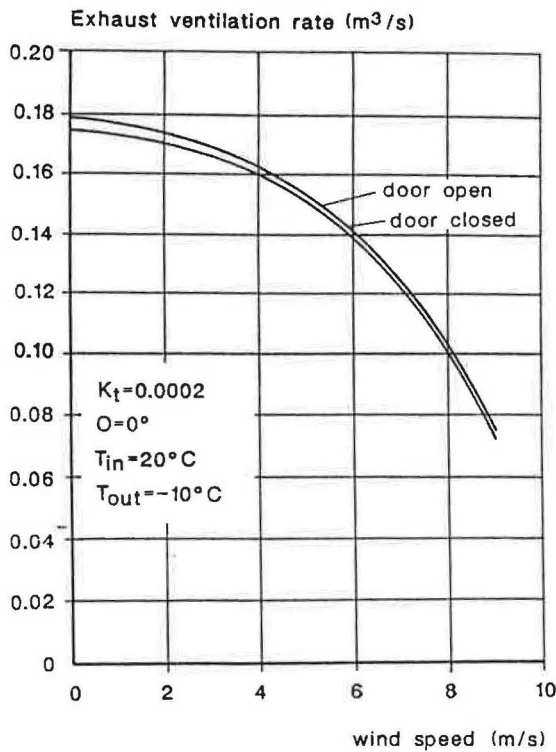


Fig. 18. The changing of the exhaust ventilation flow rates for door open and closed.

### Wind speed

The results also show that the ventilation is dominated by the exhaust system at low wind speeds, but increasingly influenced by climate at higher wind speeds. The threshold wind speed at which climate influences the ventilation rate is about 2-4 m/s, see Fig. 20. Fig. 21 shows the detailed infiltration, exfiltration, and exhaust ventilation rate with different wind speeds. There are different results for different faces of the envelope. Take, for example, the building roof, when the wind speed is less than 5-6 m/s, it is an infiltration surface, but when the wind speed is greater than 5-6 m/s, it becomes an exfiltration surface, see Fig. 21.

### Summary

The present multi-room indoor air flow model MIX can be used to calculate the infiltration, exfiltration, detailed indoor air flow, indoor pressure distribution, and interaction with the ventilation system. The single version SIX has been checked against the measurement data and has shown a good

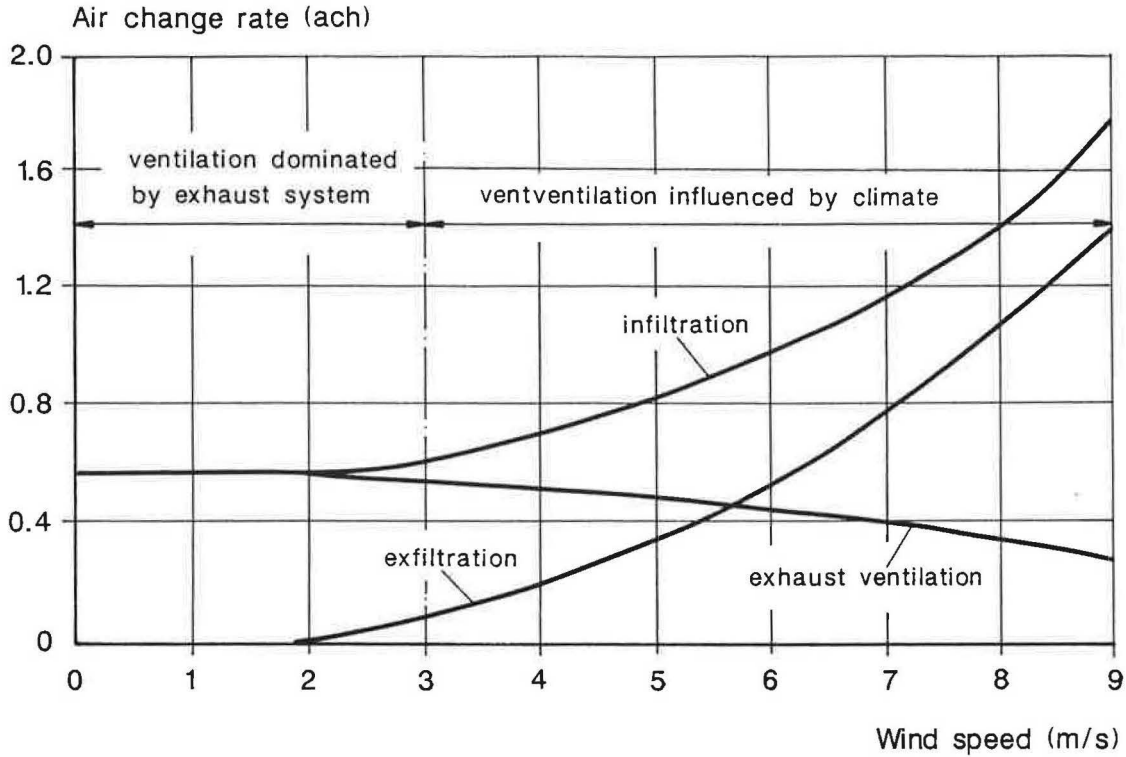


Fig. 20. Infiltration rates, exfiltration rates, exhaust ventilation flow rates for different wind speeds.

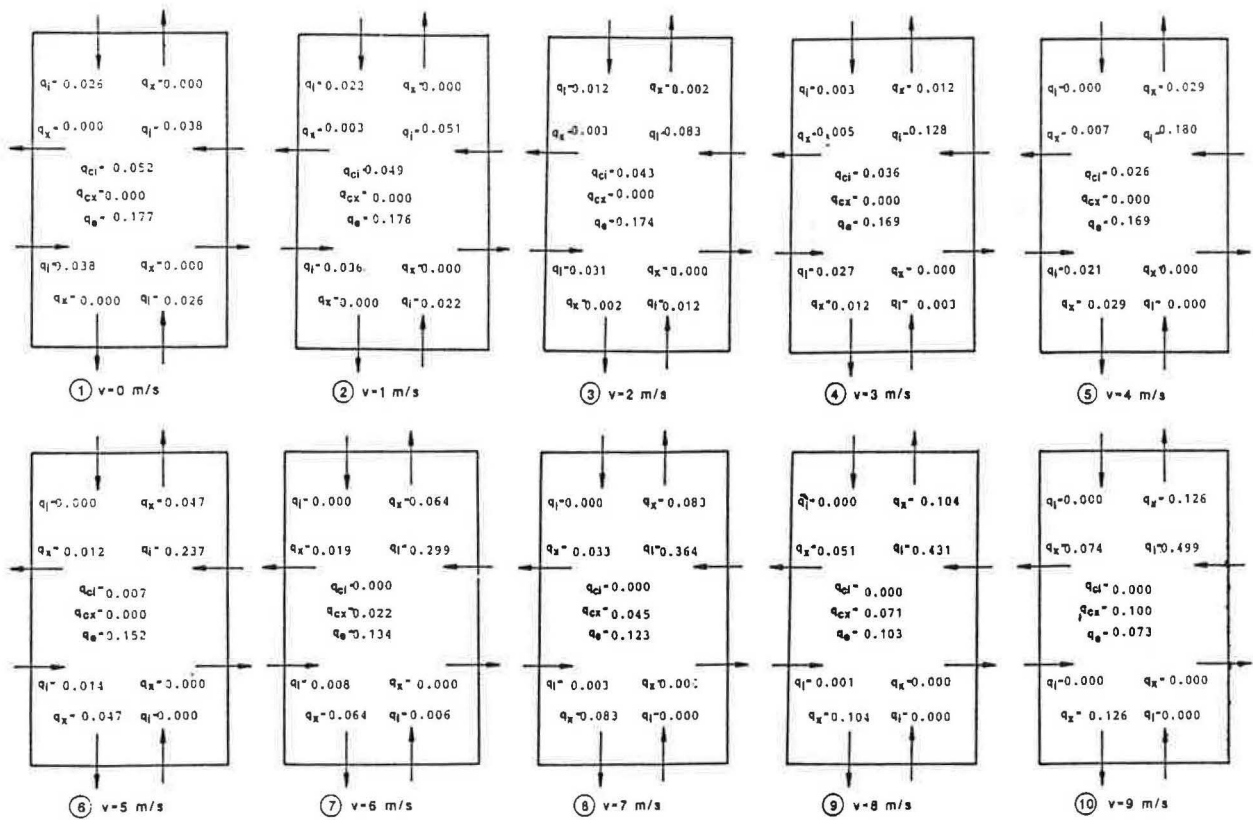


Fig. 21. Infiltration rates, exfiltration rates, and exhaust ventilation flow rates for every faces for different wind speeds.

agreement, see Li (1990). MIX will be a useful tool for further study of indoor air quality problems.

The results in the example indicate that if the openings of a multi-room building are much larger than the envelope openings there is a uniform internal pressure. In this case the single-cell model can be used. However, if the inter-room openings are smaller, then the single-cell model becomes redundant and the multi-room model should be employed.

The exhaust ventilation rate will change from the design data due to the changing of the indoor air pressure. If room pressure is above atmospheric pressure, the exhaust ventilation rate will increase, and if the indoor pressure is below the atmospheric pressure, then the exhaust ventilation rate will decrease. It has been shown that when the exhaust fan is stronger, the influence of infiltration on the exhaust ventilation system should be less.

## References

- ASHRAE Handbook: Fundamentals*, chapter 22, Natural ventilation and infiltration. ASHRAE, 1985.
- Danielson, A., Lilliengren, U., Peterson, F.:* Utomhusklimatets betydelse för den ofrivilliga ventilationen. Klimat och Byggnader, Nr 2, Institutionen för uppvärmnings- och Ventilationsteknik, KTH, 1987.
- Etheridge, D. W.:* Modelling of air infiltration in single and multi-cell buildings. *Energy and Buildings*, 10, 185-192, 1988.
- Etheridge, D. W., Alexander, D. K.:* The British gas multi-cell model for calculating ventilation. *ASHRAE Trans.*, 86, 2: 808-821, 1980.
- Feustel, H. E., Kendon, V. M.:* Infiltration models for multicellular structures- A literature review. *Energy and Buildings*, No. 8, pp. 123-136, 1985.
- Feustel, H. E., Lenz, T. P.:* Patterns of infiltration in multi-family buildings. *Building and environment*, Vol. 20, No. 1, pp. 7-13, 1985.
- Li, Y.:* Consequences of air movements in buildings. *Climate and Building*, No. 1, Dept. of Heating and Ventilation, Royal Institute of Technology, Stockholm, 1990.
- Liddament, M. W.:* Air infiltration calculation techniques-An application guide. Air infiltration centre, AIC-AG-1-86, June, 1986.
- Lilliengren, U.:* Infiltration in residential buildings. *Tekniska meddelanden*, nr 295, Vol. 16. Dept. of Heating and Ventilation, Royal Institute of Technology, Stockholm, 1986.
- Liddament, M., Allen, C.:* The validation and comparison of mathematical models of air infiltration. Air infiltration center, Technical note AIC 11, Sept., 1983.
- Shaw, C. Y.:* Methods for estimating air change rates and sizing mechanical ventilation systems for houses. *ASHRAE Trans.*, 93, 2: 2284-2302, 1987.
- Shaw, C.Y., Tamura, G.T.:* The calculation of air infiltration rates caused by wind and stack action for tall buildings. *ASHRAE Trans.*, 83, 2: 145-158, 1977.
- Sinden, F. W.:* Multi-chamber theory of air infiltration. *Building and environment*, Vol. 13, 21-28, 1978.
- Walton, G. N.:* Airflow and multiroom thermal analysis. *ASHRAE Trans.*, 88, 2: 78-91, 1982.